Int. J. Heat Mass Transfer. Vol. 19, pp. 373–384. Pergamon Press 1976. Printed in Great Britain

DIFFUSION OF HEAT AND SOLUTE DURING FREEZING OF SALT SOLUTIONS

B. W. GRANGE,* R. VISKANTA and W. H. STEVENSON
School of Mechanical Engineering, Purdue University, West Lafayette, IN 47907, U.S.A.

(*Received* 3 *June* 1975)

Abstract—An experimental and analytical investigation was made of salt redistribution phenomena which occur during the one-dimensional freezing of concentrated salt solutions. Sodium chloride solutions ranging in concentration from 0.25 to 4.0 M were frozen in a vertical test cell. A Mach–Zehnder interferometer was utilized to monitor the liquid phase concentration layer which developed ahead of the advancing solid–liquid interface. Approximate analytical solutions for the temperature and concentration distributions as well as the rate of phase change were obtained using the heat-balance integral and finite difference methods. It was found that relatively little solute is rejected from the solid–liquid interface at short times due to entrapment of the thin concentration layer by ice crystals of the advancing solid. The solute concentration at the interface is not constant but increases with time due to increased solute rejection as the opposing wall slows the interface motion. The common assumption of constant solute distribution coefficients utilized in semi-infinite domains is not valid for freezing in a region of finite thickness.

NOMENCLATURE

- C, solute concentration;
- c, specific heat capacity;
- D, mass diffusivity;
- H_f, latent heat of fusion;
- k, thermal conductivity or solute distribution coefficient (C_1/C_∞);
- k^*, solute distribution coefficient (C_1/C_i);
- L, length of finite region;
- l, thickness of test region in direction of test beam;
- N, number of fringes;
- n, index of refraction;
- St, Stefan number $(c_1/H_f)(T_i - T_0)$;
- T, temperature;
- T_f, freezing temperature of pure solvent;
- t, time;
- u, liquid bulk velocity $[1-(\rho_1/\rho_2)]\,\mathrm{d}\delta_1/\mathrm{d}t$;
- x, cartesian coordinate in direction of solid growth.

Greek symbols

- α, thermal diffusivity;
- δ_1, solid thickness;
- δ_2, liquid thickness;
- δ_3, concentration layer thickness;
- ε, distance from the interface, $x-\delta_1$;
- ρ, density;
- κ, molar freezing point depression;
- λ, wavelength of light source.

Subscripts

- 1, solid;
- 2, liquid;
- 3, concentration layer;
- i, interface;
- L, opposing wall, $x = L$;
- 0, sink, $x = 0$;
- δ_1, interface;
- ∞, infinity.

*Presently at Air Research Manufacturing Company of Arizona, Phoenix, AZ 85034, U.S.A.

1. INTRODUCTION

THERE are many problems and systems of interest in which heat and mass transfer are accompanied by a phase transformation (i.e. melting and freezing). Problems of this type are important in crystal growth from melts and solutions, freezing and melting of waters, preservation of human blood and biological specimens, solidification of castings, purification of materials, desalination of water, thermal energy storage, thermal control of spacecraft using phase change materials, and many others. For example, when a crystal is grown by oriented pulling [1] from a melt with alloyed impurities, then the impurity distribution will affect the process of impurity diffusion in the melt as well as in the solid. The overall solidification process is determined by heat and mass transfer as well as interface kinetics; whether the slow process is nucleation or growth depends on the particular system considered [2]. In many situations, however, the rate of growth is controlled by the rate at which the latent heat of fusion generated in the solidification process can be removed from the freezing front. Therefore, the knowledge of not only heat and mass transfer but also of the temperature distribution is required for more complete understanding of the solidification process.

The caracteristic feature of freezing problems is the coupling of the temperature and concentration fields with the rate of propagation of the phase boundary between the liquid and solid phases. Since both temperature and concentration as well as the coordinate of the phase boundary are unknown functions, the

problem is nonlinear. Only a few exact analytical solutions have been found for special cases [3]. Reviews of heat transfer with melting and freezing are available [4, 5]. Few experimental studies of heat and mass transfer have been performed [6–11]. Solidification of organic melts [6, 7] and of inorganic salt water solutions [8, 9] have been studied, but no temperature and concentration profiles were measured. Freezing of dilute water–sodium chloride solutions was studied [10, 11] and both temperature and concentration profiles were measured. However, the solute or impurity rejection phenomena at the solid–liquid interface is far from being understood.

This work is motivated by the need for a more complete understanding of heat and mass transfer on solidification and of solute redistribution processes in both the solid and liquid phases. To this end, a simple one-dimensional system is considered in which the diffusion of heat and solute is studied during freezing of concentrated water–sodium chloride solutions. An analysis is presented to predict the temperature and solute concentration distributions as well as the motion of the interface during one-dimensional freezing. Experiments were performed to obtain needed data. Analytical predictions are compared with experimental data to establish the validity of the analytical model and to gain understanding of the phenomena. The investigation also sheds light on the obvious question in any phase change process, i.e. how much of each phase is present at any arbitrary time after sudden application of a thermal driving force.

2. ANALYSIS

Physical model and governing equations

Figure 1 illustrates the physical model of the system. The one-dimensional region consisting of a solid and a liquid is of length L. Initially the solution is at a uniform temperature, T_L, and a uniform solute concentration, C_∞. At time $t = 0$, the temperature of the boundary at $x = 0$ is reduced to a value T_0 which is below the freezing point of the liquid. The solid begins to form and move in the x-direction. The thickness of this layer is denoted by δ_1 and the temperature in the solid and liquid regions by T_1 and T_2, respectively. The solute is less soluble in the solid, and the solute which is rejected into the liquid forms a region of increased concentration, δ_3, at the solid–liquid interface. The assumption of local thermodynamic equilibrium at the interface implies that the temperature corresponds to the equilibrium temperature for the interface concentration. The diffusion of solute and of heat are thus coupled only at the interface and are considered independent in the rest of the region.

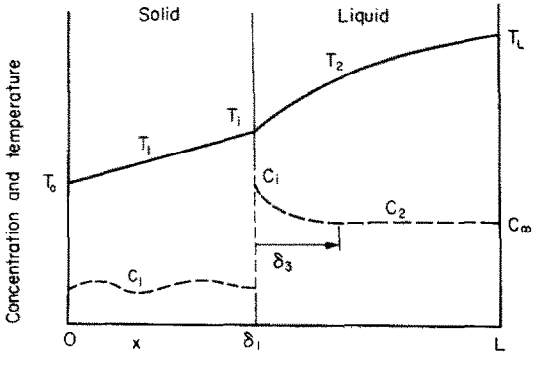

FIG. 1. Physical model and nomenclature.

The basic assumptions implied in this model are the following: (1) the system is one-dimensional, (2) the interface is of negligible thickness, (3) changes in kinetic energy are negligible and thermal radiation can be neglected, (4) local thermodynamic equilibrium exists at the interface, (5) gravitational effects are negligible, (6) physical properties are constant, (7) thermal diffusion and diffusion-thermo effects are negligible in comparison to molecular diffusion, and (8) solution and solid are chemically inert.

The equations describing the processes in the two regions include the diffusion of energy and of solute in the solid and liquid are the following:

Solid (Region 1):

$$\rho_1 c_1 \frac{\partial T_1}{\partial t} = \frac{\partial}{\partial x}\left(k_1 \frac{\partial T_1}{\partial x}\right) \tag{1}$$

and

$$C_1 = C_1(t). \tag{2}$$

The concentration in the solid is a function of the solidification rate, interface kinetics, and interface morphology which usually must be specified from experimental data.

Liquid (Region 2):

$$\rho_2 c_2 \frac{\partial T_2}{\partial t} + \rho_2 c_2 [1-(\rho_2/\rho_2)] \frac{\mathrm{d}\delta_1}{\mathrm{d}t} \frac{\partial T_2}{\partial x} = \frac{\partial}{\partial x}\left(k_2 \frac{\partial T_2}{\partial x}\right) \tag{3}$$

and

$$\frac{\partial C_2}{\partial t} + [1-(\rho_1/\rho_2)] \frac{\mathrm{d}\delta_1}{\mathrm{d}t} \frac{\partial C_2}{\partial x} = \frac{\partial}{\partial x}\left(D \frac{\partial C_2}{\partial x}\right). \tag{4}$$

The term $[1-(\rho_1/\rho_2)]\mathrm{d}\delta_1/\mathrm{d}t$ represents the bulk velocity of the liquid normal to the interface due to the difference in densities of the two phases.

An energy balance at the interface obtained by equating the net energy flux leaving the interface to the latent heat released during solidification results in

$$k_1 \frac{\partial T_1}{\partial x}\bigg|_{\delta_1} - k_2 \frac{\partial T_2}{\partial x}\bigg|_{\delta_1} = \rho_1 H_f \frac{\mathrm{d}\delta_1}{\mathrm{d}t}. \tag{5}$$

As a result of the motion of the interface [12], equation (5) is nonlinear and thus the difficulty in obtaining solutions is greatly increased.

If the solid and liquid phases have different densities, the boundary at $x = L$ must be permeable to allow liquid to pass during the formation of a solid. A species balance is made by equating the initial solute to that which is in the ice, the liquid, and that which passes through the boundary at $x = L$ due to bulk movement. For times smaller than that necessary for the concentration layer to reach $x = L$, the species balance results in

$$\int_{\delta_1}^{L} (C_2 - C_\infty)\,\mathrm{d}x = \int_0^{\delta_1} [(\rho_1/\rho_2)C_\infty - C_1]\,\mathrm{d}x. \tag{6}$$

The initial, boundary, and interface conditions are:

$$\begin{aligned} &T_2(x,0) = T_L \quad \text{and} \quad C_2(x,0) = C_\infty \\ &T_1(0,t) = T_0 \qquad\quad C_1(t) \text{ specified} \\ &T_1(\delta_1,t) = T_i \\ &T_2(\delta_1,t) = T_i \qquad\quad C_2(\delta_1,t) = C_i \\ &T_2(L,t) = T_L \qquad\quad C_2(L,t) = C_\infty. \end{aligned} \tag{7}$$

The interface temperature and concentration are coupled by the assumptions of local thermodynamic equilibrium and of the freezing point depression being proportional to concentration at the interface,

$$T_i = T_f(1-\kappa C_i). \tag{8}$$

Thus the problem is to solve the partial differential equations (1), (3) and (4) utilizing the auxiliary equations (5), (6) and (8) with the initial and boundary conditions (7) to find $T_1(x,t)$, $T_2(x,t)$, and $C_2(x,t)$ for $0 < x < L$, $t > 0$. The nonlinearity due to the moving boundary and a region of finite extent exclude an exact analytical solution. Since the governing equations are not amenable to exact solutions, two approximate techniques were utilized.

Finite difference method

The first technique considered was a finite difference method. In order to solve the governing equations numerically, an implicit method was utilized which allowed a close nodal spacing near the interface without requiring unacceptably small time steps for numerical stability.

Since the diffusion of energy is orders of magnitude faster than that of solute diffusion, it was necessary to use two separate nodal systems. A single nodal system for both the energy and species conservation equations would have resulted in a system which was either adequate for temperature and too crude for concentration, or adequate for concentration and too fine for temperature and would have resulted in prohibitive computer time. As a result, the energy equations utilized a nodal system over the entire x-domain while a fine mesh grid was used only in the solute rich region for the conservation of solute equation. As the finite difference solution advanced in time, the concentration layer increased in thickness, included larger numbers of nodes, and thus increased the required computer time per time increment, Δt. Therefore, the number of concentration nodes within the concentration layer was constantly monitored and if the number of nodes exceeded 48, the nodal spacing was doubled thereby decreasing the number of nodes by a factor of two. Forty-one temperature and a minimum of 12 concentration nodes were used at any given time during the solution. This allowed an accurate determination of the temperature and concentration profiles while utilizing acceptable time increments and computer time. Details of the computational scheme are given by Grange [13].

Whereas the solute concentration in the solid has been observed to remain constant with time for solidification in a semi-infinite domain, it is a complicated function of the interface velocity and interface temperature gradients during solidification in a finite domain. As a result, it was necessary to utilize experimental solid concentration data in the solute balance, equation (6), for comparison of the temperature and liquid concentration profiles.

Because the interface temperature is related to the interface concentration by equation (8), a numerical instability was observed at the interface. A small error in the solute balance would result in a small change in the solidification temperature which influenced the interface location. The result was an unstable oscillating interface temperature and concentration. By constraining the interface concentration to change by no more than 5% in any one time increment, very good agreement was obtained with the exact solution [10] for constant solid concentration and a semi-infinite domain.

As in all finite difference solutions of Stefan-type problems, some error is introduced when initiating the numerical procedure. The error arises from the necessity of having a finite amount of solid initially present to start the procedure. This error has always been observed to diminish or become negligible as the solution proceeded in time.

Integral method

In order to examine the significance of various parameters, an approximate solution was obtained using the integral method of Goodman [14]. In this procedure the temperature and concentration distributions are approximated by polynomials with coefficients which are functions of time. The governing equations are integrated over the x-domain thus reducing the partial differential equations to ordinary differential equations in time. Boundary conditions are used to determine all but one of the coefficients in each polynomial which are then determined by solving the system of ordinary differential equations. The integral method of solution has the advantage of requiring an order of magnitude less computer time than the finite difference method of solution for typical boundary conditions examined.

By integrating equation (1) from $x = 0$ to $x = \delta_1$ and equations (3) and (4) from $x = \delta_1$ to $x = L$, there results

$$\alpha_1\left(\frac{\partial T_1}{\partial x}\bigg|_{\delta_1} - \frac{\partial T_1}{\partial x}\bigg|_0\right) = \frac{\partial}{\partial t}\int_0^{\delta_1} T_1\,\mathrm{d}x - T_i\frac{\mathrm{d}\delta_1}{\mathrm{d}t} \tag{9}$$

$$\int_{\delta_1}^{\delta_1+\delta_3}\left[\alpha_2\frac{\partial^2 T_2}{\partial x^2} - u\frac{\partial T_2}{\partial x}\right]\mathrm{d}x = \int_{\delta_1}^{\delta_1+\delta_3}\frac{\partial T_2}{\partial t}\mathrm{d}x \tag{10}$$

and

$$\int_{\delta_1}^{\delta_1+\delta_3}\left[D\frac{\partial^2 C_2}{\partial x^2} - u\frac{\partial C_2}{\partial x}\right]\mathrm{d}x = \int_{\delta_1}^{\delta_1+\delta_3}\frac{\partial C_2}{\mathrm{d}t}\mathrm{d}x \tag{11}$$

respectively.

Approximating the temperature distribution in the solid by a first order polynomial in x and both the temperature and concentration profiles in the liquid by

third order polynomials in x results in the following expressions [13]

$$\frac{T_1-T_0}{T_i-T_0}=x/\delta_1 \tag{12}$$

$$\frac{T_2-T_i}{T_L-T_i}=(1+2h)\left(\frac{x-\delta_1}{\delta_2}\right)-3h\left(\frac{x-\delta_1}{\delta_2}\right)^2+h\left(\frac{x-\delta_1}{\delta_2}\right)^3 \tag{13}$$

$$\frac{C_2-C_\infty}{C_i-C_\infty}=3\left(\frac{x-\delta_1}{\delta_3}\right)-3\left(\frac{x-\delta_1}{\delta_3}\right)^2+\left(\frac{x-\delta_1}{\delta_3}\right)^3. \tag{14}$$

A linear approximation for the temperature of the solid is adequate if the thermal diffusivity of the solid is sufficiently larger than that of the liquid. From analysis and experiment [10], it is clear that this is an excellent approximation for the H_2O–NaCl solutions considered in this investigation.

The assumption of a constant solute concentration in the solid is valid for solidification in a semi-infinite domain [10] but, as will be discussed, it is not valid for solidification within a finite domain. The approximation of a constant solute concentration in the solid is utilized, however, as it allows a qualitative examination of freezing in a finite domain without requiring prior knowledge of the concentration profile in the solid.

Utilizing the interface energy balance, equation (5), to couple the solid and liquid phases and substituting the assumed profiles into equation (9), results in an ordinary differential equation for δ_1,

$$\frac{\mathrm{d}\delta_1}{\mathrm{d}t}=\frac{\alpha_1\left(\frac{1}{\delta_1}-\frac{k_2}{k_1}\frac{1+2h}{\delta_2}\frac{T_L-T_i}{T_i-T_0}\right)+\frac{1}{2}\frac{\delta_1}{(T_i-T_0)}\frac{\mathrm{d}T_i}{\mathrm{d}t}}{\frac{\alpha_1\rho_1 H_f}{k_1(T_i-T_0)}+\frac{1}{2}}. \tag{15}$$

In a similar manner, for the liquid region the resulting equation for the coefficient h becomes

$$\frac{\mathrm{d}h}{\mathrm{d}t}=4\left\{\alpha_2\left[\frac{1-h}{\delta_2^2}-\frac{k_1(T_i-T_0)}{k_2(T_L-T_i)\delta_1\delta_2}\right]+\left[\frac{\alpha_1\rho_1 H_f}{k_2(T_L-T_i)}+\left(\frac{\rho_1}{\rho_2}-\frac{1}{2}+\frac{1}{4}h\right)\right]\frac{1}{\delta_2}\frac{\mathrm{d}\delta_1}{\mathrm{d}t}-(\tfrac{1}{2}-\tfrac{1}{4}h)\frac{1}{T_L-T_i}\frac{\mathrm{d}T_i}{\mathrm{d}t}\right\}. \tag{16}$$

Introducing equation (14) and the boundary conditions into equation (11) results in

$$\frac{\mathrm{d}\delta_3}{\mathrm{d}t}=4\left[\frac{3D}{\delta_3}-\frac{\rho_1}{\rho_2}\frac{\mathrm{d}\delta_1}{\mathrm{d}t}-\frac{1}{4}\frac{\delta_3}{(C_i-C_\infty)}\frac{\mathrm{d}C_i}{\mathrm{d}t}\right]. \tag{17}$$

An overall solute balance, equation (6), yields an expression for the interface concentration

$$C_i=C_\infty+4(\delta_1/\delta_3)[(\rho_1/\rho_2)C_\infty-C_1]. \tag{18}$$

Taking the time derivative of equation (18) and substituting into equation (17) results in

$$\frac{12D}{\delta_3}=4\left(\frac{\rho_1}{\rho_2}+\frac{\delta_3}{\delta_1}\right)\frac{\mathrm{d}\delta_1}{\mathrm{d}t}. \tag{19}$$

Note that $\mathrm{d}\delta_3/\mathrm{d}t$ has been eliminated from the equation. Since $\delta_3/\delta_1 \ll 1$, the expression for δ_3 simplifies to

$$\delta_3=3D\Big/\left(\frac{\rho_1}{\rho_2}\right)\frac{\mathrm{d}\delta_1}{\mathrm{d}t}. \tag{20}$$

Because $\mathrm{d}\delta_3/\mathrm{d}t$ is needed to determine the interface temperature–time derivative, $\mathrm{d}T_i/\mathrm{d}t$, which is required to determine δ_1 and h, there are not enough equations to determine all the unknowns. Physically $\mathrm{d}T_i/\mathrm{d}t$ is small and a good approximation to the solution can be obtained by neglecting the term. The interface temperature is then obtained by substituting equation (18) and (20) into equation (8) with the result

$$T_i=T_f\left[1-\kappa C_\infty-\tfrac{4}{3}\frac{\kappa}{D}\frac{\rho_1}{\rho_2}\delta_1\frac{\mathrm{d}\delta_1}{\mathrm{d}t}\left(\frac{\rho_1}{\rho_2}C_\infty-C_1\right)\right]. \tag{21}$$

The freezing time can be thought to consist of two basic time periods. During the first period the boundary temperature at $x=L$ has no influence on the liquid temperature profile and the semi-infinite domain solution is valid. After the calculated temperature difference at $x=L$ exceeds 2%, i.e. $|[T_2(L,t)-T_L]/(T_i-T_L)|>0.02$, the integral solution is utilized. The 2% temperature differential was arbitrarily selected as corresponding to the time at which the boundary temperature, T_L, begins to influence the liquid temperature profile. Equations (15) and (16) were solved utilizing a fourth-order Runge–Kutta algorithm. A constant time increment, Δt, of one second was used and the results compared with the finite difference solutions to confirm convergence and stability.

Comparison of methods of solution

Because no comparable exact or approximate analysis exists, except for short times, it was not possible to determine precisely what magnitude of error could be expected from the numerical calculations. An estimate of the accuracy of the two methods was made by comparing the finite difference solution to the exact semi-infinite domain solution at short times and comparing the integral and finite difference solutions for later times. Although the accuracy of either method by itself was unknown, the probability of two entirely different methods giving identically wrong answers should be very small.

Two sample problems were solved utilizing the integral and finite difference methods of solution to compare the results. The first example consisted of pure water and did not involve solute rejection. For short times the integral method of solution utilizes the exact solution for the Stefan problem [12]. A comparison of the results is shown in Tables 1 and 2. Two general trends are evident in the finite difference result. First, since a finite amount of solid must be present to start the numerical procedure, an initial error is introduced into the predicted solid thickness (Table 1). The error is observed to decrease rapidly with time. Secondly, with the solidification temperature specified, any error introduced into the predicted solid thickness will result in erroneous temperatures near the interface. Thus, the

Table 1. Comparison of solid thicknesses based on exact and finite difference solutions for the solid thickness of pure water: $T_L = 275\,K$, $T_0 = 160\,K$, $\rho_1/\rho_2 = 1.0$, $L = 10\,cm$

	Solid thickness, δ_1 (cm)		
Time (s)	Exact	Finite difference	Difference (percent)
1.0	0.110	0.123	11.0
5.0	0.247	0.274	10.9
10.0	0.349	0.386	10.6
50.0	0.780	0.804	3.1
100.0	1.10	1.12	1.8
500.0	2.47	2.47	0.0

Table 2. Comparison of temperatures based on exact and finite difference solutions for the temperature profiles of pure water: $T_L = 275\,K$, $T_0 = 160\,K$, $\rho_1/\rho_2 = 1.0$, $L = 10\,cm$

	Temperature (K)			
	$x = 0.5\,cm$		$x = 1.0\,cm$	
Time (s)	Exact	Finite difference	Exact	Finite difference
1.0	275.000	274.985	275.000	274.9999
5.0	274.998	274.887	275.000	274.999
10.0	274.839	274.654	275.000	274.993
50.0	236.133	234.639	274.579	274.403
100.0	214.796	214.048	263.998	262.590
500.0	184.860	184.782	209.187	209.032

Table 3. Comparison of solid thicknesses based on integral and finite difference solutions for the solid thickness with solute rejection: $T_L = 294.4\,K$, $T_0 = 238\,K$, $C_\infty = 1.0\,mol/l$, $C_1 = 0.915\,mol/l$, $\rho_1/\rho_2 = 0.92$, $L = 10\,cm$

	Solid thickness, δ_1 (cm)		
Time (s)	Integral	Finite difference	Difference (percent)
300	0.854	0.89	−4.0
600	1.21	1.25	−3.3
1200	1.71	1.76	−2.9
1500	1.95	1.96	−0.7
2400	2.52	2.48	1.6
3600	3.09	3.04	1.6
4800	3.56	3.51	1.4
6000	3.97	3.92	1.2
7200	4.34	4.29	1.1

Table 4. Comparison of temperatures based on integral and finite difference solutions for the temperature profiles with solute rejection: $T_L = 294.4\,K$, $T_0 = 238\,K$, $C_\infty = 1.0\,mol/l$, $C_1 = 0.915\,mol/l$, $\rho_1/\rho_2 = 0.92$, $L = 10\,cm$

	Temperature (K)			
	$x = 1.0\,cm$		$x = 5.0\,cm$	
Time (s)	Integral	Finite difference	Integral	Finite difference
300	272.598	271.084	294.400	294.3996
600	262.106	261.199	294.387	294.367
1200	255.148	254.600	293.787	293.655
2400	249.111	249.771	284.481	289.432
3600	247.061	247.623	280.488	284.325
4800	245.865	246.355	276.738	279.736
6000	245.053	245.489	273.455	275.844
7200	244.452	244.824	270.650	272.522

Table 5. Comparison of concentration layer thicknesses based on integral and finite difference solutions for concentration layer thickness with solute rejection: $T_L = 294.4\,K$, $T_0 = 238\,K$, $C_\infty = 1.0\,mol/l$, $C_1 = 0.915\,mol/l$, $\rho_1/\rho_2 = 0.92$, $L = 10\,cm$

	Concentration layer thickness, δ_3 (cm)		
Time (s)	Integral	Finite difference	Difference (percent)
1800	0.051	0.053	3.8
3000	0.065	0.067	3.0
4200	0.077	0.083	7.2
5400	0.095	0.087	−9.2
6600	0.119	0.122	2.4
7800	0.149	0.152	2.0
9000	0.189	0.191	1.0

error in temperature is observed to be greatest in the region of the interface and also decreases with time. The results indicate that the finite difference procedure compares excellently with the exact analytical solution except at $t \to 0$.

The second example consisted of a 1.0 M-sodium chloride solution and included solute rejection. A comparison between the finite difference results and the two part integral solution are presented in Tables 3–5 and Fig. 2. This example illustrates two additional features that result from solute rejection. First, as a

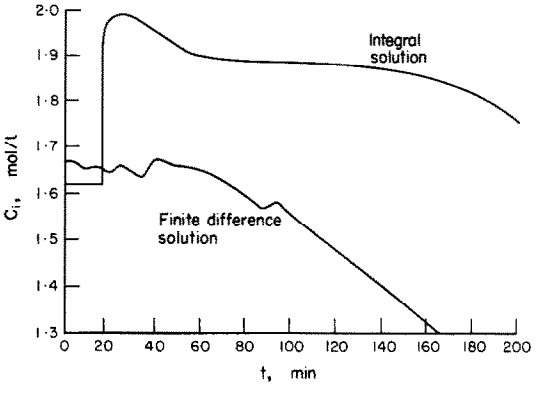

FIG. 2. Comparison of liquid interface concentrations: $T_L = 294.4\,K$, $T_0 = 238\,K$, $C_\infty = 1.0\,mol/l$, $C_1 = 0.915\,mol/l$, $\rho_1/\rho_2 = 0.92$, $L = 10\,cm$, $H_f = 3.35 \times 10^5\,J/kg\,K$.

consequence of the assumed concentration profile in the second part of the integral solution, there is a sudden increase in the predicted interface concentration (Fig. 2). The interface concentration is varied such that the species balance, equation (7), is satisfied when applied to the approximate concentration profile rather than to the exact profile utilized in the first part of the solution. The sudden increase is due solely to the difference in the concentration profiles utilized in the solution.

The thickness of the concentration rich solute layer predicted by the two methods are in excellent agreement if δ_3 is defined as the distance from the interface to the location $(C_2 - C_\infty)/(C_i - C_\infty) = 0.05$. Since the finite difference solution approximates an exponential profile, extending an infinite distance from the interface,

it is necessary to define δ_3. As a result of doubling the concentration node spacing, previously discussed, a relatively large difference, 9.2%, is noted at 5400 s. The difference is observed to diminish rapidly after the change in spacing.

3. EXPERIMENTS

To obtain needed data and to verify the analytical model, temperature and concentration profiles were measured during the solidification of saline ($NaCl$–H_2O) solutions. The liquid concentration profiles were measured with a Mach–Zehnder interferometer of conventional design utilizing a monochromatic (He–Ne laser) light source. Concentrated saline solution was chosen as the test medium because the solution is nearly transparent in the visible part of the spectrum and the change in index of refraction is much more sensitive to concentration than to temperature changes [13, 15].

Test cell

A schematic diagram of the test cell employed in the study is shown in Fig. 3. Optical glass plates, installed perpendicular to the interferometric test beam, constituted two of the sides of the test cell while sheets of Plexiglas were used to make up the remaining two sides. Two 1.27 cm thick gold-plated copper heat sinks measuring $9.16 \times 2.35 \times 1.27$ cm formed the top and bottom of the test cell. The internal dimensions of the test region were $3.75 \times 2.35 \times 6.1$ cm. Small Plexiglas spacers were used to construct an air gap which acted as a barrier to heat gain through the Plexiglas walls. Outside the glass walls a 0.63 cm air gap containing silica gel was used to reduce heat loss and to prevent frost or condensation.

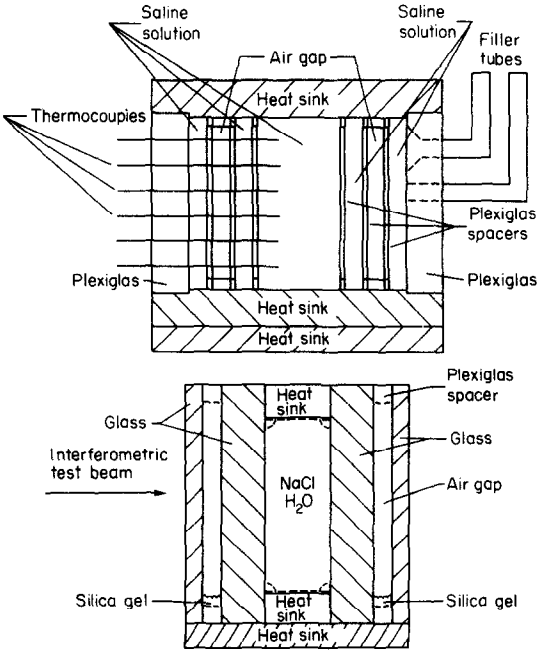

FIG. 3. Schematic diagram of test cell.

Two 0.76×0.89 cm channels were milled in each heat sink for coolant flow. A larger $9.16 \times 8.38 \times 1.27$ cm copper heat sink was located below the smaller one to reduce the thermal load on the smaller one and to cool the lower edge of the glass wall. This was necessary to minimize wall effects and heat gain through the relatively thick optical glass sides. The test cell was held together by two metal brackets located at the top and bottom. The top, bottom, and sides were then covered with asbestos insulation. Reference can be made to Fig. 3 for further details of the construction.

The top heat sink was maintained at a constant temperature using a Lauda TK 30D Ultra Kryomat with ethylene glycol as the coolant. The lower heat sinks were initially brought to steady state with the Lauda TK30D circulator. An experimental run was initiated by switching the lower heat sinks to a different system consisting of a Lauda NBSD 8125 Circulator and a dry ice heat exchanger with ethyl alcohol as the coolant.

Instrumentation

Temperatures were measured at fixed points with type K Chromel–Alumel thermocouples made from 30 gauge wire equally spaced along the length of the test region. Thermocouples were located at the mid-point and end of each of the gold plated heat sinks, 0.051 cm below the surface. Two thermocouples were also located in the external coolant for use in controlling the coolant temperature. Thermocouple e.m.f. were recorded using a 20 channel recording Doric Integrating Digital Voltmeter.

Test procedure

The test procedure consisted of bringing the brine solution in the test region to a uniform temperature. The interferometer was adjusted until an infinite fringe was present. The dry ice system was precooled and switched into the lower heat sinks to approximate a step temperature drop. A cathetometer was used to determine the ice thickness and fringe patterns were recorded on film periodically through the run. A number of experimental runs were made with initial NaCl concentration varying between 0.25 and 4.0 M. The temperatures of the cold and hot heat sinks were held constant at approximately 238 and 294 K, respectively.

Data reduction

Because the diffusion of heat is approximately two orders of magnitude faster than the diffusion of mass the temperature profile in the region of the concentration layer was approximately linear. As a result, the concentration profile was obtained from the recorded interferogram by first examining a region outside the concentration layer to obtain the fringe density due to temperature effects alone. The measured fringe density was then subtracted from the fringe pattern within the concentration layer. The resulting fringe pattern was

due to concentration gradients only and the concentration was obtained from

$$C_2 = C_\infty + (N\lambda/l)/(\partial n/\partial C)_T. \quad (22)$$

The variation of index of refraction with concentration was determined at the bulk concentration from the data measured and presented in [13].

4. RESULTS AND DISCUSSION

Several observations were made during the experimental runs which should be mentioned prior to discussing the experimental results.

Wall effect became very important at late times when heat gain from the surroundings affected the flatness of the interface. Heat gain through the glass walls resulted in a thin layer of liquid remaining between the solid and glass in the region of the interface. This layer allowed the dense, highly concentrated solution near the interface to flow by gravity into this region. Therefore, the actual interface concentration was higher than experimentally determined.

The quality of the ice improved as the initial bulk concentration was lowered. Pure water and dilute solutions formed a clear or a white translucent solid while the 2.0 and 4.0 M solutions formed a gray solid. The effect of de-gassing by boiling was shown quite vividly for pure water. Unboiled water resulted in small projections or air worms on the surface of the ice which were absent for the de-gassed water.

Accurate determination of the interface location proved to be difficult due to a thin transparent layer of ice at the interface. This layer's thickness was of the order of interface movement between measurements at late times.

The analytical program consisted of two parts. First, the governing equations were solved numerically using a finite difference method and the predictions were compared with the experimental data. This physical model simulates the unsteady one-dimensional heat and mass transfer and allows for a time dependent concentration in the solid. Second, the integral method of solution was used to obtain approximate temperature and concentration profiles and to examine the influence of important physical parameters. A limitation of the integral method is that a constant (time-independent) concentration of the salt in the solid was assumed. The approximation is acceptable since only a relative influence was sought, and most importantly, computer time requirements were considerably reduced.

Comparison of experimental data with predictions

Tests were conducted with initial sodium chloride solutions of 0, 0.25, 0.50, 1.0, 2.0 and 4.0 M. The initial bulk temperature and wall temperature were 294 and 238 K, respectively, in each experimental run. Two to four runs were performed at each concentration to confirm repeatability for the procedure and data. Here, only sample results are presented for the 2.0 M. The complete results are given elsewhere [13].

Typical temperature distributions as a function of position with time as a parameter are shown in Fig. 4.

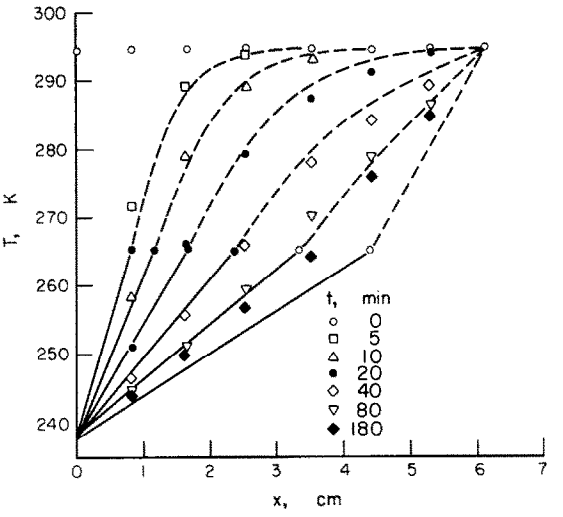

FIG. 4. Comparison of predicted and measured temperatures for solidification of 2.0 M-NaCl: $T_0 = 238$ K, $T_L = 294$ K, $L = 6.1$ cm.

The comparisons between predicted (using the finite difference method of solution) and measured temperature profiles show good agreement. The greatest discrepancies occur at late times and are mainly caused by heat gain through the walls and sides of the test cell. As expected, this energy gain results in smaller measured ice thicknesses than predicted analytically and correspondingly higher measured temperatures. Other sources of discrepancy include the finite time required to reduce the sink temperature and the inability to maintain the cold sink temperature constant.

Terwilliger and Dizio [10] and others [16, 17] have shown the concentration in the solid and at the interface to be constants during solidification in a semi-infinite region. The solute concentrations at the interface and in the solid, however, are not constant during freezing in a region of finite extent but vary with time. Except for a simple energy balance, the solutions do not model the interface kinetics. For this reason the experimentally determined values of the solute concentration in the solid, C_1, were used in the finite difference solute balance, equation (6).

A comparison of measured and predicted dimensionless solute concentration profiles in the liquid is presented in Fig. 5. Although the shapes of the measured and predicted concentration profiles agree well, they differ near the outer edge of the concentration layer. This is a result of substituting as a function of time the experimentally measured solid concentration data in the species balance, equation (6), of the finite difference solution. Heat gains from the surroundings resulted in greater analytically predicted solid thickness than the measured one at any given time. Thus, the analysis predicts a greater solute content in the concentration layer than experimentally measured. The measured and predicted interface concentrations agree quite closely as shown in Fig. 6.

Since the greatest discrepancy between the data and the exponential profile was in the region where the

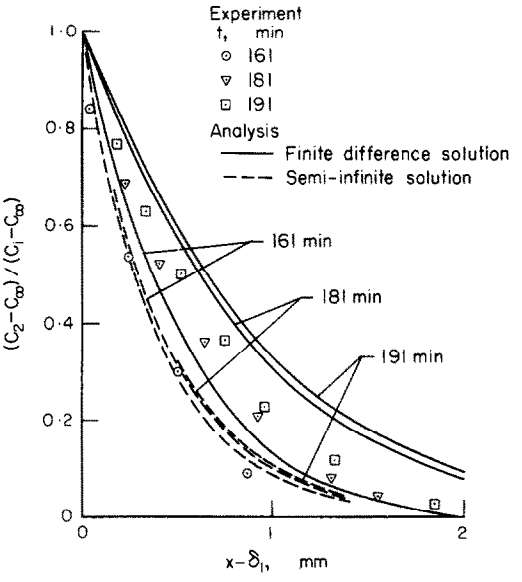

FIG. 5. Comparison of predicted and measured dimensionless liquid concentration during solidification of 2.0 M-NaCl: $T_0 = 238$ K, $T_L = 294$ K, $L = 6.1$ cm.

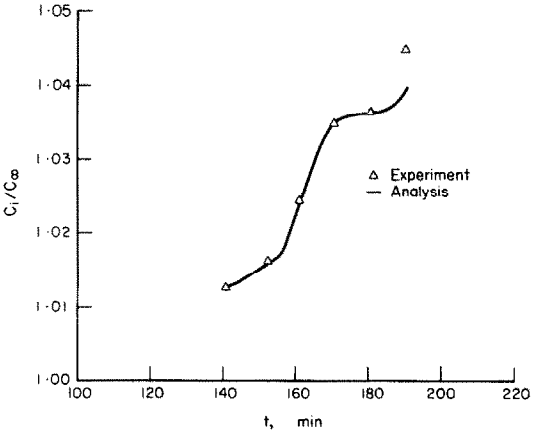

FIG. 6. Comparison of predicted and measured dimensionless liquid interface concentration during solidification of 2.0 M-NaCl: $T_0 = 238$ K, $T_L = 294$ K, $L = 6.1$ cm.

concentration profile approached the initial concentration, the concentration layer was arbitrarily defined as the distance from the interface where the change in concentration has reached 5% of its maximum value, i.e. $(C_{\delta_3}-C_\infty)/(C_i-C_\infty) = 0.05$. The concentration layer was then determined by a least squares fit of the experimental data. The measured solute concentration profiles in the liquid, when plotted in dimensionless form, approximate an exponential decrease quite closely, Fig. 7. The dimensionless concentration profiles collapse onto a single curve which is only a function of the dimensionless distance from the interface. This relationship implies that there is no characteristic length in the problem and the solutions are "similar". The similarity solution [10] for the semi-infinite domain is illustrated in Fig. 5. It is evident that the concentration layer for a finite region expands more

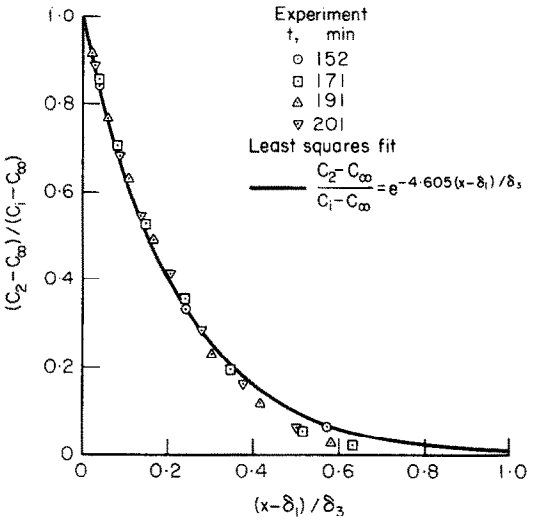

FIG. 7. Dimensionless liquid concentration vs dimensionless distance from the interface during solidification of 2.0 M-NaCl: $T_0 = 238$ K, $T_L = 294$ K, $L = 6.1$ cm.

quickly due to the slowing down of the interface. Since the interface velocity is not proportional to $t^{\frac{1}{2}}$, a similarity constant for solidification within a finite domain cannot be obtained analytically.

The solute distribution in the solid is an important parameter indicating the solute rejection efficiency of the interface. At early times when the interface velocity was relatively large, little or no solute rejection was observed. This is believed due to the small amount of solute rejected initially which formed either a concentration layer which was too thin to be observed or so thin it was entrapped by the advancing ice crystals on a microscopic level. At later times, when solute rejection became significant, the interface velocity was very small. Although the solute in the concentration layer could be measured quite accurately, errors in determining the amount of solid which had formed between observations (± 0.05 mm) resulted in large errors in the measured solute concentration distributions in the solid. For use in the finite difference model, an average solute concentration in the solid was determined based upon the total ice thickness.

Important parameters previously used in solidification studies are the distribution coefficients $k = C_1/C_\infty$ and $k^* = C_1/C_i$. For semi-infinite domains each of these parameters remains a constant [10, 16, 17] while in a finite domain they both vary with time [13]. Due to the inaccurate solute concentration data in the solid, no quantitative values can be given for k and k^*. Both parameters decrease with time once an observable concentration layer is formed as C_1 decreases and C_i increases with time. The value of k^* must eventually reach a minimum and then increase as C_i must return to the ultimate bulk concentration when steady state is approached.

Comparison of predicted and measured ice thicknesses as functions of time are shown in Fig. 8. The experimentally measured ice thickness lags the predicted thickness due to heat gain into the test cell.

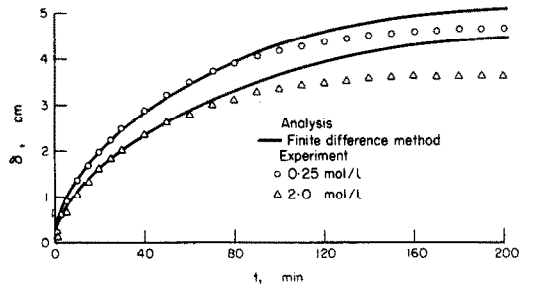

FIG. 8. Comparison of predicted and measured solid thickness for $C_\infty = 0.25$ and 2.0 M-NaCl: $T_0 = 238$ K, $T_L = 294$ K, $L = 6.1$ cm.

Influences of important physical parameters

In order to examine the influence of various parameters the integral solution was utilized. This method has the advantage of requiring an order of magnitude less computer time than the finite difference solution while having the disadvantage of assuming the solute content of the solid is constant. The reference conditions considered consisted of a region 10 cm long with boundary temperatures $T_0 = 238$ K and $T_L = 294$ K, and a 1.0 M solution. The following property data were used in the calculations:

Solid

$$k_1 = 2.22\,\text{J/m s K}$$
$$\alpha_1 = 1.15 \times 10^{-6}\,\text{m}^2/\text{s}$$
$$\rho_1 = 920\,\text{kg/m}^3$$

Liquid

$$k_1 = 6.03 \times 10^{-1}\,\text{J/m s K}$$
$$\alpha_2 = 1.44 \times 10^{-7}\,\text{m}^2/\text{s}$$
$$\rho_2 = 1000\,\text{kg/m}^3$$
$$D = 9 \times 10^{-10}\,\text{m}^2/\text{s}$$
$$H_f = 3.35 \times 10^5\,\text{J/kg K}.$$

For a given system, varying the sink temperature, T_0, greatly affects the resulting temperature profile and ice thickness, see Fig. 9. Decreasing the sink temperature, T_0, increases the interface velocity. The result is an increase in the interface concentration of approximately 50% and a decrease in the interface temperature of approximately 4 K for $T_0 = 200$ K.

The effect of solute concentration in the solid on the temperature profile is shown in Fig. 10. A very small, 1.7%, decrease in the solute concentration of the ice increases the concentration at the interface by nearly 78% causing a decrease in the interface temperature and ice thickness. The solute content of the solid is very important in understanding the response of the system.

Freezing in a region of finite extent is contrasted to freezing in a semi-infinite region by the affects of the opposing wall temperature, T_L, upon the rejection of solute at the solid–liquid interface. However, even if the salt concentration in the solid is constant during freezing in a region of finite extent the liquid interface concentration varies with time once the opposing wall

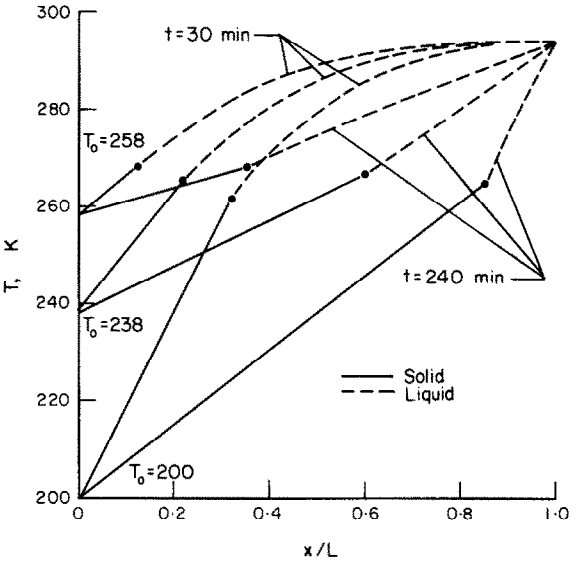

FIG. 9. Effect of sink temperature, T_0, on temperature distribution: $C_\infty = 1.0$ mol/l, $C_1 = 0.915$ mol/l, $T_L = 238$ K, $L = 10$ cm.

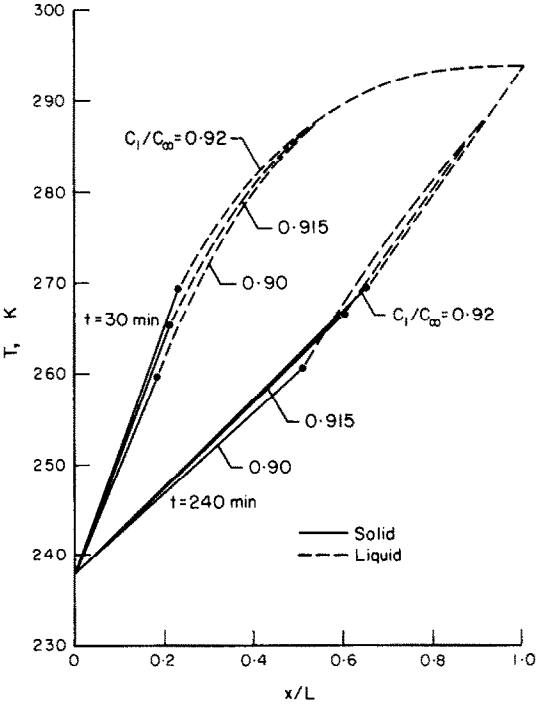

FIG. 10. Effect of solid–liquid concentration ratio on temperature distribution: $C_\infty = 1.0$ mol/l, $T_0 = 238$ K, $T_L = 294$ K, $L = 10$ cm.

temperature, T_L, influences the temperature gradients at the interface.

Several parameters are important in determining the interface concentration. A small decrease in the solute concentration in the solid increases the interface concentration greatly due to the relatively slow diffusion of solute in the liquid. The sensitivity of the interface concentration to solute concentration in the solid is illustrated in Fig. 11. Likewise, if the sink temperature, T_0, is decreased, causing the solid to form

Table 6. Effect of sink temperature, solid solute concentration, and Stefan number on the concentration layer thickness, δ_3: $C_\infty = 1.0$ mol/l, $C_1 = 0.915$ mol/l, $T_0 = 238$ K, $T_L = 294$ K, $St = 0.176$, $L = 10$ cm

	δ_3 (cm)				
Time (min)	Reference condition	$T_0 = 258$ K	$T_0 = 200$ K	$C_1/C_\infty = 0.92$	$C_1/C_\infty = 0.90$
20	0.0323		0.0278	0.0389	
30	0.0446	0.0697	0.0308	0.0405	0.0575
40	0.0539	0.0896	0.0368	0.0492	0.0652
60	0.0690	0.118	0.0462	0.0631	0.0829
90	0.0859	0.149	0.0567	0.0785	0.103
120	0.0966	0.173	0.0678	0.0912	0.119
150	0.113	0.193	0.0832	0.104	0.134
180	0.128	0.213	0.104	0.119	0.148
210	0.144	0.234	0.135	0.137	0.164
240	0.163	0.256	0.184	0.159	0.181

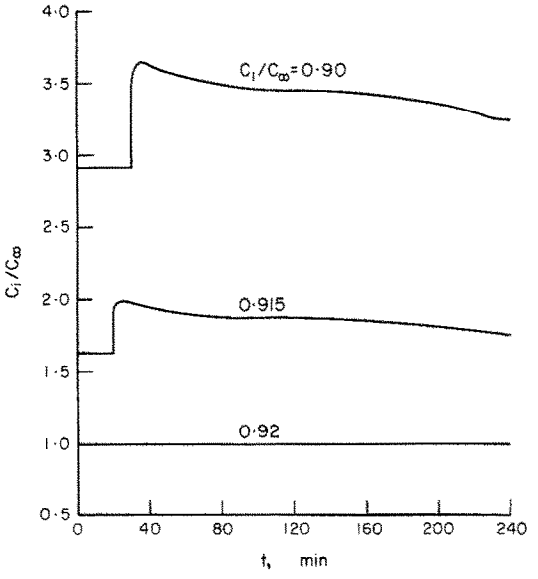

FIG. 11. Effect of solid–liquid concentration ratio on interface concentration: $C_\infty = 1.0$ mol/l, $T_0 = 238$ K, $T_L = 294$ K, $L = 10$ cm.

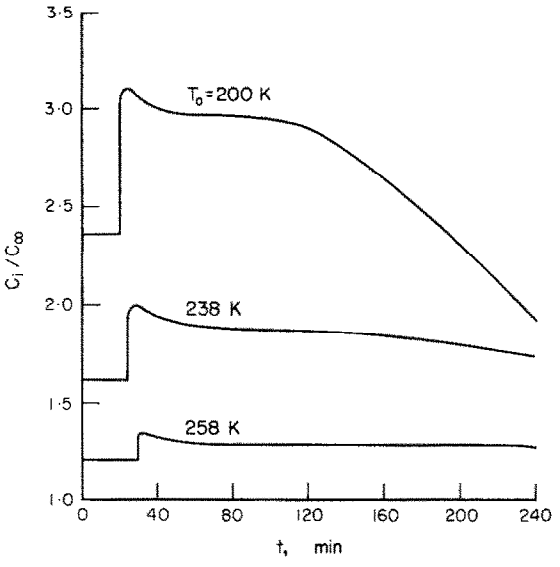

FIG. 12. Effect of sink temperature, T_0, on interface concentration: $C_\infty = 1.0$ mol/l, $C_1 = 0.915$ mol/l, $T_L = 294$ K, $L = 10$ cm.

more rapidly, the increased time rate of solute rejection into the liquid increases the interface concentration, Fig. 12.

Table 6 summarizes the predicted concentration layer thickness, δ_3, for variations in parameters compared with the assumed reference conditions. It is noted that the integral solution yields a value of δ_3 even if there is no solute rejection (i.e. $C_1/C_\infty = 0.92$).

5. CONCLUSIONS

Solute redistribution during freezing in a finite domain differs greatly from freezing in a semi-infinite domain. Based upon the results of this investigation the following conclusions can be drawn: (1) The liquid interface concentration is not constant but increases with time due to increased solute rejection. The solute rejection increases due to the influence of the opposing wall in slowing the interface. The integral solution utilizing the incorrect assumption of C_1 constant yields the opposite result. The common assumption of constant solute distribution coefficients (k, k^*) utilized in semi-infinite domains is invalid for freezing in a region of finite length. (2) The mechanisms controlling solute rejection may change during solidification in a finite region. Relatively little solute is rejected from the solid–liquid interface at short times due to entrapment of the thin concentration layer by ice crystals of the advancing solid. Bulk entrapment at the interface accounts for the majority of the solute in the solid, but the amount of entrapment could not be predicted. Until a more complete understanding and modeling is achieved, the concentration distribution of the salt in the solid must be furnished as an input parameter for analysis. It appears that a complete description of the solute rejection must be based on the microscopic effects occuring at the interface. The effects of concentration, gravity, temperature gradients, and crystal orientation must be understood before the salt rejection phenomena at the interface can be explained. Application of nonequilibrium thermodynamic concepts to the freezing of solutions may be a fruitful area of future research.

Acknowledgements—Partial financial support to carry out this research was provided by NSF-MRL Program Grant GH-33574. National Science Foundation provided financial support to one of the authors (B. W. Grange) in the form of a traineeship.

REFERENCES

1. R. L. Parker, Crystal growth mechanisms: energetics, kinetics and transport, in *Solid State Physics*, edited by E. Ehrenreich, *et al.*, Vol. 25, pp. 151–299. Academic Press, New York (1970).
2. J. W. Mullin, *Crystallization*. CRC Press, Cleveland (1972).
3. L. I. Rubinstein, in *The Stefan Problem, Trans. Math. Monogr.*, Vol. 27. American Mathematical Society, Providence (1971).
4. S. G. Bankoff, Heat conduction or diffusion with a phase change, in *Advances in Chemical Engineering*, edited by T. B. Drew, *et al.*, Vol. 5, pp. 75–150. Academic Press, New York (1964).
5. J. C. Muehlbauer and J. E. Sunderland, Heat conduction with freezing and melting, *Appl. Mech. Rev.* **18**, 951–959 (1965).
6. M. Matsouka, T. Hayakawa and S. Fujita, Fundamental study of fractional solidification: effect of heat transfer rate on crystal growth rate, *Heat Transfer—Japan. Res.* **1**, 58–64 (1972).
7. T. Hayakawa and M. Matsouka, Effect of heat transfer on crystal growth for inorganic salt–water systems, *Heat Transfer—Japan. Res.* **2**, 104–115 (1972).
8. T. Hayakawa and M. Matsouka, Studies of unidirectional crystal growth as the basis of normal freezing, *J. Chem. Engng Japan* **7**, 180–186 (1974).
9. T. Hayakawa, M. Matsouka and K. Satake, Phenomena of solidification in normal freezing of a simple eutectic forming organic melt, *J. Chem. Engng Japan* **6**, 332–337 (1973).
10. J. P. Terwilliger and S. F. Dizio, Salt rejection phenomena in the freezing of saline solutions, *Chem. Engng Sci.* **25**, 1331–1348 (1970).
11. B. W. Grange, R. Viskanta and W. H. Stevenson, Solute and thermal redistribution during freezing of salt solutions, in *Heat Transfer* 1974, Vol. 1, pp. 220–224. JSME/MSChE, Tokyo (1974).
12. H. W. Carslaw and J. C. Jaeger, in *Conduction of Heat in Solids*, 2nd edn, p. 282. Oxford University Press, London (1959).
13. B. W. Grange, Diffusion of heat and solute during freezing of salt solutions, Ph.D. Thesis, Purdue University, West Lafayette, Indiana (1975).
14. T. R. Goodman, Application of integral methods to transient nonlinear heat transfer, in *Advances in Heat Transfer*, edited by T. F. Irvine and J. P. Hartnett, Vol. 1, pp. 51–122. Academic Press, New York (1964).
15. J. A. Wasatjerna, Losnintars optiska egerskaper, *Acta Soc. Sci. Fenn*: Ser. A **50** (1920).
16. W. A. Tiller, K. A. Jackson, J. W. Rutter and B. Chalmers, The redistribution of solute atoms during the solidification of metals, *Acta Metall.* **1**, 428–437 (1953).
17. P. P. Zolotarev, Theory of the freezing process in thick layers of solutions, *J. Appl. Mech. Tech. Phys.* **7**, 106–108 (1966).

DIFFUSION DE CHALEUR ET DE MASSE LORS DE LA CONGELATION DE SOLUTIONS SALINES

Résumé—Une étude expérimentale et analytique est effectuée sur le phénomène de redistribution du sel qui se produit lors de la congélation unidimensionnelle de solutions salines concentrées. Des solutions de chlorure de sodium, de concentrations molaires allant de 0,25 à 4,0, sont congelées dans une cellule verticale. Un interféromètre Mach–Zehnder est utilisé afin de suivre, en phase liquide, la couche de concentration qui se développe au dessus de l'interface solide–liquide en progression. Des solutions analytiques approchées des distributions de température et de concentration, aussi bien que de la vitesse de changement de phase, sont obtenues à l'aide de l'intégrale du bilan thermique et de méthodes aux différenoes finies. On trouve qu'une quantité relativement faible du soluté est rejetée de l'interface solide–liquide pendant des intervalles de temps courts, car la fine couche de concentration se trouve piégée par les cristaux de glace du solide qui progresse. La concentration du soluté à l'interface augmente avec le temps, fait dû à l'augmentation du rejet de soluté lorsque la paroi opposée ralentit le mouvement de l'interface. L'hypothèse habituelle de coefficients constants de la distribution du soluté, utilisée dans les domaines semi-infinis, ne s'applique pas à la congélation dans un domaine d'épaisseur finie.

DIFFUSION VON WÄRME UND FLÜSSIGKEIT WÄHREND DES GEFRIERENS VON SALZLÖSUNGEN

Zusammenfassung—Es wurde eine experimentelle und analytische Untersuchung durchgeführt über die Wiederverteilungsprobleme von Salz während des eindimensionalen Gefriervorgangs von konzentrierten Salzlösungen. In einer senkrechten Versuchszelle wurden Kochsalzlösungen im Konzentrationsbereich von 0,25 bis 4,0 molar gefroren. Ein Mach–Zehnder Interferometer wurde benützt, um die flüssige Phase der Konzentrationsschicht anzuzeigen, die sich vor der fortschreitenden Festfront entwickelte. Analytische Näherungslösungen für die Temperatur- und Konzentrationsverteilungen sowie für die Geschwindigkeit der Phasenänderung wurden mit Hilfe eines Wärmebilanzintegrals und der Methode finiter Elemente erhalten. Es zeigte sich, daß relativ wenig Lösungsmittel von der Festgrenze abgewiesen wird bei kurzen Zeiten, da die Eiskristalle der fortschreitenden Festfront für den Einschluß der dünnen Konzentrationsschicht sorgen. Die Konzentration des Lösungsmittels an der Trennfläche ist nicht konstant, sondern nimmt mit der Zeit zu, da die gegenüberliegende Wand die Geschwindigkeit des Fortschreitens der Trennfläche verzögert und zu einer erhöhten Abweisung des Lösungsmittels führt.

Die für halbunendliche Bereiche übliche Annahme einer konstanten Verteilung der Lösungskoeffizienten gilt nicht für den Gefriervorgang in Bereichen endlicher Dicke.

ДИФФУЗИЯ ТЕПЛА И РАСТВОРЕННОГО ВЕЩЕСТВА ПРИ ЗАМЕРЗАНИИ СОЛЯНЫХ РАСТВОРОВ

Аннотация — Проведено экспериментальное и теоретическое исследование явлений перераспределения солей при одномерном замерзании концентрированных соляных растворов. В экспериментальном вертикальном сосуде замораживались растворы хлористого натрия, концентрация которых изменялась от 0,25 до 4,0 молей/литр. Интерферометр Маха–Цендера использовался для визуализации концентрационного слоя в жидкости, который развивался перед движущейся поверхностью раздела фаз твердое тело-жидкость. Были получены приближенные аналитические решения для распределений температуры и концентрации, а также с помощью конечно-разностных методов и интеграла теплового баланса была рассчитана скорость фазового перехода. Найдено, что относительно небольшое количество растворенного вещества отводится с поверхности раздела твердое тело-жидкость за короткий промежуток времени благодаря захвату тонкого концентрацнонного слоя кристаллами льда на движущейся твердой поверхности. На поверхности раздела фаз концентрация растворенного вещества непостоянна, а увеличивается временем за счет увеличения количества удаленного от твердой поверхности растворенного вещества, так как противоположные стенки замедляют движение поверхности раздела. Общее допущения о постоянстве коэффициентов распределения растворенного вещества, используемых в полубесконечных областях, несправедливо для случая замерзания в области конечного размера.